Chapter 2

Experimental Methods in the Study of Neutron Scattering at Small Angles

Cristian A. Dragolici

Additional information is available at the end of the chapter

http://dx.doi.org/10.5772/62184

Abstract

Scattering methods are powerful tools used for the examination of condensed matter. They offer the possibility to analyze particles without disturbing their natural environment. Small angle neutron scattering (SANS) can also be used to analyze solid and liquid systems, phase transformations, germination, growth flaws and defects, as well as generally any inhomogeneity occurring in a range of 10–1000 Å. The most common experimental SANS methods and patterns are reviewed and explained.

Keywords: SANS, methods, patterns

1. Introduction

1.1. Material science issues accessible through small angle scattering of X-rays (SAXS) and neutrons (SANS)

The fundamental properties of the neutron make it a powerful tool for materials science investigations. It is useful to introduce neutrons by comparison with X-rays because both probes are used for diffraction investigations, and more workers are familiar with X-ray methods. X-rays can be obtained with a generator tube or, in the past few years, at a synchrotron X-ray laboratory.

Neutrons for neutron beam research arise either from nuclear fission in reactors or from the spallation process. In the latter, accelerator-produced high-energy charged particles yield a large number of energetic neutrons from collisions with heavy-atom nuclei in the accelerator target.

X-ray diffraction was utilized for the first time in establishing the atomic structure of the crystals. Later, this method was used in other applications, extended to the study of imperfections in crystals, of the size of the crystallites, and even to the study of amorphous objects. From the classical discovery by Laue, in 1912, that X-rays are diffracted on their passage through crystals, the development of the applied domain of this technique was due to the subsequent progress of the X-ray diffraction theory and the improvement of experimental methods. The first observations on small angle X-ray scattering (SAXS) were performed in the beginning of the 1930s [1], and its domain was developed later.

In the following years, the small angle X-ray scattering technique has known to be an important development, proved by a great number of publications over the years. SAXS technique was developed from the necessity to observe long lattice spacing in crystals, in comparison with wavelengths of the X-rays used in structural analyses. Such distances are encountered in certain minerals and certain complex molecules such as polymers or proteins. For example, in the study of macromolecular crystals, the systems for X-ray diffraction should be extended to include the very small angles. The fundamental equation which describes the X-ray diffraction in the crystalline substance is $\boldsymbol{\lambda = 2d\sin\theta}$, which shows that the diffraction angle θ inversely varies with the separation distance of the crystalline lattice planes (see Fig. 1) which generates the considered diffraction maximum.

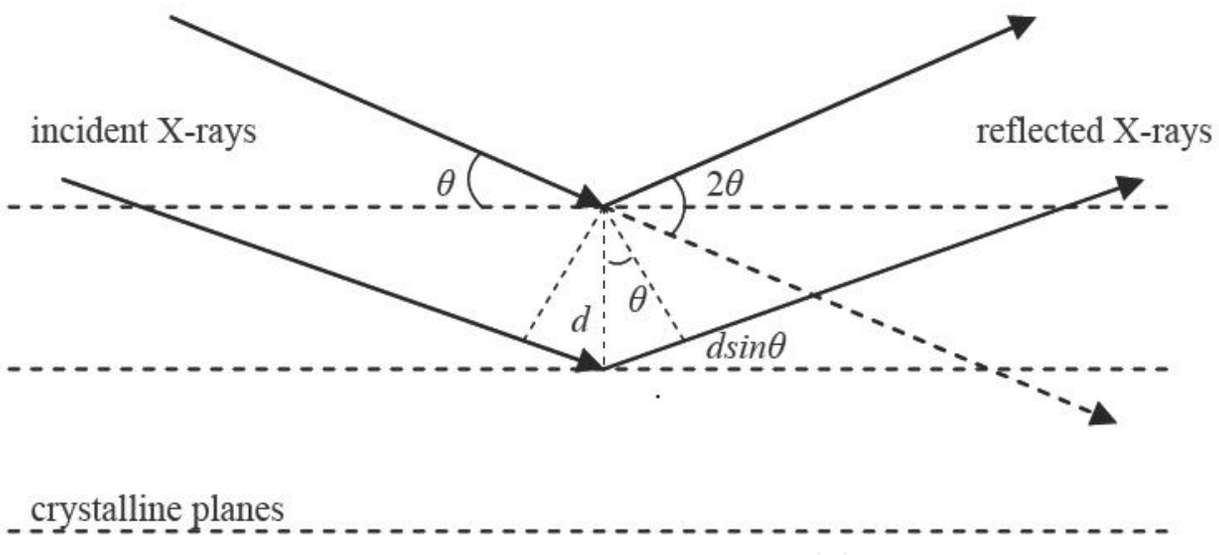

Figure 1. Bragg diffraction of the X-rays.

In ordinary crystals, especially those of inorganic matter, most inter-lattice distances observed are on the same magnitude with the wavelength of utilized X-rays; therefore the used θ angles are quite large. For example, let us consider the radiation Cu k_α and an inter-lattice distance of 100 Å, which would result in a diffraction θ angle of 0.45°; for a distance of 1000 Å, θ would be 0.045° or 2.6′. All these examples had shown the importance of SAXS techniques in biology, biochemistry, etc. Using X-rays with long wavelength to obtain larger diffraction angles for a specific inter-lattice distance is strictly limited by the variation of the material X-ray linear

http://dx.doi.org/10.5772/62184

absorption coefficient with radiation wavelength. Because X-rays are strongly absorbed by the traversed substance, it also became necessary for the utilization of other particles with higher penetrability due to their weak interaction with the matter they are passing through. Elsasser first observed in 1936 that neutron movement could be determined by wave mechanism, and later two experiments were conducted by Halban and Preiswerk and Mitchell and Powers, respectively, which validated this theory [2]. These experiments were performed using source emitting neutrons of different energies, without considering collimation or monochromation of that beam. However, all these conditions were sufficient to emphasize the neutron diffraction but without providing quantitative data. The development of nuclear reactors made possible the availability of neutrons in a very large number to allow collimation in beams, and separation by energy in a narrow band. This was the beginning of the neutron diffraction technique, very similar to X-ray diffraction.

The first device of this type, initially called "neutron spectrometer," was built for the first time in 1945 at Argonne National Laboratory in USA. Since then, many instruments with different shapes and conception were built around the world, and they are mostly known as "neutron diffractometer." The investigation of condensed matter with the help of neutrons is not a substitute for classical X-ray diffractions, but it is a completion of these techniques, because the special nature of neutron interaction with the substance allows the neutron diffraction to provide information that cannot be revealed by other means. The spectrum of neutrons emitted by a reactor is dependent on the moderator temperature, and in most reactors, the spectrum peak is around 1.5 Å. This spectrum is Maxwellian and has a maximum which depends on the temperature. Therefore, for T = 273 K, λ_{max} is around 1.55 Å, and for T = 373 K λ_{max} is 1.33 Å. Using "hot sources," it is possible to move the maximum of the neutron spectrum to short wavelengths up to 0.4 Å. In a similar manner, by cooling the moderator, the maximum of the neutron spectrum can be moved to long wavelengths. We can observe that neutron beams, as spectrum broadening, become comparable with X-ray beams, where the normal range of wavelengths is from 2.2 Å (Cr K_α) to 0.56 Å (Ag K_α), thereby having the advantage of being less absorbed by the matter than X-rays. In the last years, in the competition between X-rays and neutrons, the synchrotron sources have been developed without compromising on the advantages of neutron diffraction. Today, the progress of X-rays and thermal neutron radiation sources makes it possible to use diffraction experiment radiations with λ up to 10 Å, and the development of the technology to obtain crystals with "pre-established inter-lattice" distances assures the conditions to extract monochromatic beams from the radiation emitted by the source. In their competition with X-rays, the neutrons have the huge advantage of being less absorbed by the matter in comparison with X-rays, which allow them to be used in the investigation of not only volume effects but also surface effects. In the case of neutrons, there are two ways of interaction with condensed matter, with the nuclei or with the atomic magnetic moments of the investigated material. Over the years, several methods were developed to investigate the partial order of analyzed systems. Among these methods, the technique of small angle neutron scattering is the most valuable. Technically speaking, the term "small angle scattering" (SAS) does not refer always to small diffraction angles but to small values of the quantity Q which is the scattering vector, $\vec{Q} = \vec{k} - \vec{k}_0$, where $\vec{k}_0$ and $\vec{k}$ are the wave vectors of the incident and scattered radiations. For elastic scattering $Q = (4\pi/\lambda)\sin\theta$, where θ is half of the

scattering angle and λ is the radiation wavelength. In the angular range of SAS, the interested intensity is produced by inhomogeneities extended from 10 to 1000 Å. The quantity D of these inhomogeneities determines the most interesting angular range [3]:

$$\frac{1}{D} < Q < \frac{10}{D}$$

There are many processes that lead to scattering length variations, extended to zones up to 100 Å. Among these, there are the processes in solid phase namely aging, precipitating processes in solid phase, repeated thermal shock, neutron irradiation, the processes in mixed systems, for example the catalysts, where the two coexisting solid crystalline components are of enormous interest, as well as the ferofluids or the polymers in which neither one component is crystalline. The application of SAXS and SANS to material science has its origin from the experiments performed by Guinier in 1938, to study different types of aluminum alloys with various components such as Al–Cu and Al–Ag. He proved the existence of extremely small precipitate zones (so-called Guinier–Preston (GP) zones) as the first step in solidification of the precipitate of these alloys [3]. The GP zones represent submicroscopic regions of the matrix in which are produced a concentration of the initial solvate element. From one point of view, the GP zones could be considered as pre-precipitates because their formation represents a preliminary stage of precipitations set up from ultra-saturated matrix, but from another point of view it could be considered "clusters," in the sense that represent preferential associations of atoms.

In Al–Cu alloys, it has a diameter of about 80 Å and a thickness of 3–6 Å. With an average composition of 90% Cu, it comes out that the GP zones in these alloys are predominant constituted from Cu atoms. The physical nature and structural characteristics of the formed precipitates are dependent on temperature and heating duration because the precipitates are formed by germination and growing up processes, based on diffusion phenomena. The most important modification of alloy proprieties occur in the initial stages of the aging, with low temperatures and short heating durations when microstructural transformations are to a scale size under the resolution limit of optical microscopy (submicron precipitates). All these phenomena could be emphasized by SAXS and SANS methods. Regrouping of various atoms species during the precipitation process modifies the dispersion strength of X-rays or neutrons in different zones of aged alloy, due to the existence of an important density difference between the precipitated zones and the rest of alloy matrix. Among the structural processes produced through thermal treatment, which is applied to solid crystalline materials, the spinodal transition is something special [3]. The first phases of coherent precipitation took place through phase separation inside the crystalline lattice. Phase separation could start only through a nucleation process followed by nuclei growing. The germination of a new phase in a solid solution needs that in some regions the solid solution should considerably modify its composition. To be transformed into stable germs, these regions should have a specific dimension (about 10 Å). In these conditions, the interface between the germ and the solid solution (matrix) shows a distinct structural discontinuity, and therefore it has a free positive energy which

http://dx.doi.org/10.5772/62184

inhibits the germination. This germination difficulty is more evident in spinodal decomposition. In this case, the matrix regions, where the composition is modified, became more extended than classical germs and are named clusters. The interface between the matrix and the regions with modified composition became diffusive and does not present anymore a distinct structural discontinuity characterized by a positive free energy. To produce regions with modified composition, extended on large volumes, long-range composition fluctuations are necessary that would tend to decompose the original solid solution. The probability of these long-range composition fluctuations is much more increased when the temperature of original solid solution is situated close to the alloy "spinodal temperature." Above the spinodal temperature T_s (where the second derivative of the Gibbs free energy for the solid solution is positive), the supersaturated solid solution is metastable. Below the T_s spinodal temperature, the second derivative of the Gibbs free energy is negative, resulting in an unstable solid solution, which separates immediately by spinodal decomposition. Concentration fluctuations of spinodal transition are detected by their geometrical parameter values, in SAS methods structural observation domain. By these methods, it can be defined as a wavelength λ_c and obviously its reciprocal $Q = 2\pi/\lambda_c$ that depend on different factors as temperature difference ($T_s - T$) or energy gradient. Cahn provided a quantitative description of the primary phase's kinetics of spinodal decomposition, in his linear approximation theory. In accordance with this theory, the growing rate has a maximum for the wavelength $\lambda_m = 2^{1/2}\lambda_c$. Thus both wave vectors Q_c and Q_m can be experimentally deduced by SAS because the intensity $I(Q)$ is proportional with the amplitude square of the suitable concentration waves. SAS methods provide quantitative information not only about particle dimensions but also about volume fraction of the second phase as well as metastable mixture limits. Therefore, the idea of using SANS as a nondestructive testing method for the industry came to reality. Because neutron absorption in the substance is very low, machine components of relatively large thickness can be easily investigated by SANS. The initial steps in this direction began in Italy by a research group from Fiat Corporation. They built a cold neutron source for different material studies. They began in 1974 when Pizzi and coworkers performed several tests on various materials used in machine components and spare parts [3]. For example, they tested the palettes of a turbine that works for a very long time in a power plant. The base material was a Ni alloy, with the particle dimensions between 200 and 300 Å, which confer some mechanical properties to that alloy. After 16,000 of hours working time, they noticed a radial growth of the constituent particles, in the middle and top of the palettes, reaching 900 Å when the breaking occurred after approximately 60,000 working hours. Similar effects were observed in the aviation turbine palettes, where the heavy working conditions affected the particles situated mostly in the middle of the palettes. Other tests were carried out on different machine parts built of heterogeneous materials subject to cyclic deformations or having areas affected by strong heating (welding zones). The conclusion was that any change in the dimension of constituent particles (up to 1000 Å) could be easily observed using the SANS technique. Another field of SAS applicability is the study of flows (voids) appearing in some materials irradiated with neutrons [3]. The components of nuclear reactors are subject to massive exposure to high rapid neutron fluxes, therefore resulting in the necessity of the determination and study of defects that might appear in those materials, having effects on the modification of initial proprieties.

The stress yielding of the material is correlated with the occurrence of a high concentration of micropores having a diameter between 200 and 1000 Å. Pores having smaller dimensions (≤ 25 Å) are usually present in a very large number and influence the material density. The intermediary sized pores give the gas permeability and the stability to irradiation of the covering layers. All these become visible by SAS technique utilization. SANS is a very useful instrument in the study of microscopic distribution of the magnetic field and the static interaction of spins from different magnetic system as well. Magnetic scattering is caused by the interaction between the neutron magnetic moment and the local magnetization of the sample. If this occurs at a small Q, it will show the magnetization fluctuations adequate for large distances in the studied sample and also the magnetic periodicities extended on large distances.

Another important field of study is offered by complex disordered materials such as ceramics, clays, cement, or glasses. Among these, the importance of cement in modern society cannot be underestimated. Cement is found in concrete structures everywhere such as buildings, roads, bridges, dams, and even for conditioning radioactive wastes. There is no escape from the impact of cement in our everyday life. Due to its great importance in the following, we will point only on its applications. Cement, as it is commonly known, is a mixture of compounds made by burning limestone and clay together at very high temperatures ranging from 1400 to 1600°C. Water is the key ingredient, which when mixed with cement forms a paste that evolves as a hard product. The water causes the hardening of the cement by a process called hydration. Hydration is a chemical reaction in which the major compounds in cement form chemical bonds with water molecules to yield hydrates or hydration products.

The heterogeneous nature and chemical complexity of the cement make the characterization of this system difficult. In spite of the inherent difficulties of the system, considerable understanding of the nature of cement and concrete has been obtained through the use of a wide variety of tools.

Studies of the cement pore liquid as a function of time, X-ray diffraction investigations, electron microscope, and NMR experiments have all contributed to a better understanding of the behavior of this material.

The greater penetrating power of neutrons (in comparison to X-rays), the opportunities for in situ measurement of hydrating pastes, the ability to use very long wavelength incident neutrons and the unique opportunities to change contrast offered by D_2O–H_2O exchange make SANS attractive as a means to probe the internal microstructure of cement pastes. The issue to be resolved, however, is the interpretation of the small angle scattering data. While the actual measurements are generally straightforward, the complexity of phases, contrasts, object morphologies, and size ranges forms a barrier to simple interpretations.

Small angle neutron scattering was first used to study the microstructure of cements in the early 1980s by Allen and coworkers [4]. They measured the small angle neutron scattering from a set of cement specimens hydrated at different water to cement ratios. They also examined the effect of soaking the specimen in heavy water and the change in SANS obtained when the specimen was dried. In their analysis of the SANS data, they assumed a simplified

model of the cement hydration reactions. In this model, the hydrated compounds C_6AFH_{12}, C_4AH_{13}, C_3ACSH_{12}, and $C_3S_2H_{2.5}$ and the hydroxides $Mg(OH)_2$, $Ca(OH)_2$, NaOH, and KOH in appropriate amounts were the products of cement hydration. Each of these compounds represented a different volume fraction of the cement paste. The strength of the SANS signal from the specimen in the small Q Guinier region was directly proportional to the square of the scattering length density difference (the contrast, see Equation 18) and to the total volume of the scattering particles. If the scattering in the two-phase model is to be interpreted as between the matrix $C_3S_2H_{2.5}$ and pores in the $C_3S_2H_{2.5}$ gel, it matters whether the pores are filled with light water, heavy water, or with air. The contrast between $C_3S_2H_{2.5}$ and water will vanish where the scattering length density curves intersect, at approximately 60% D_2O. If SANS data from cement paste are to be interpreted on the basis of a two-phase model, one issue is the identification of the appropriate phases. While the contrast is proportional to the SANS intensity, the detailed shape of the SANS curves will depend on the size distribution and shape of the scattering objects.

The SANS is presumed to be caused by a size distribution of objects of a known shape. To calculate the form factor for objects of known shape we can use Equation 17.

The parameters describing the object and its size distribution are then varied to minimize the difference between the calculated scattering and the data. Spheres, cylinders, and disks were considered by Allen and coworkers, and it was ultimately concluded that the SANS from their cement paste specimens was created by a distribution of water-filled spherical pores approximately 5 nm in diameter and a smaller component of pores with diameters of about 10 nm. SANS from the specimen that had been dried and not rewetted was interpreted as the one due to scattering from a much broader distribution of pore sizes with a peak of about 5 nm but extending to much larger diameters.

SANS from the specimens immersed in D_2O showed that the heavy water rapidly exchanged with the water in the pores and with the water in the surrounding C–S–H gel. The total porosity was of the order 1% of the volume.

All these are only a few examples that illustrate the large field of SAS application, where the immediate observation of the phenomena produced in materials lead to solving many practical problems and to extend the theoretical knowledge as well.

2. Physical principle of SANS

SANS is a method used to obtain information regarding the shape, dimensions, and internal configuration of the zones with scattering density significantly different from the average value, having relatively small dimensions (up to 1000 Å), unevenly distributed in some environment, where the distance arrangement is present or not. In a considered sample, all scattering centers participate in the scattering process. The scattering centers could be atoms, molecules, or particles of the analyzed system. System response could be a spatial distribution of scattered radiation reducible to a succession of maximums, determined by the existence of

distance arrangement in a material, or a succession of overlapping maximums over a continuous distribution when the distance arrangement is accompanied by disordered processes, such as amorphization, precipitation in solid phase, flaws, etc., or by a continuous distribution which present one or two isolated maximums like in the case of liquids (in this case the maximum is owed to the next close vicinity of each scattering center) or a continuous curve in case of SANS. Because X-ray scattering is similar to neutron scattering, in the following presentation I will start with the theoretical principles of SAXS accordingly adapted for SANS. It is well known that a diffraction image of a sample could be easily described in terms of reciprocal space or Fourier space [1]. If we consider $\rho(\vec{x})$ as the electronic density of the scattering body in a point defined by the vector $\vec{x}$, then $A(\vec{Q})$ is defined as the transform of $\rho(\vec{x})$ in the point defined by the vector $\vec{Q}$ in the reciprocal space, and it is given by

$$A\left(\vec{Q}\right) = \int \rho\left(\vec{x}\right) \exp\left(-i\vec{Q}\cdot\vec{x}\right) d\vec{x} \tag{1}$$

The X-ray diffraction theory is based on the fact that $A(\vec{Q})$ represents the amplitude of scattered radiation when $\vec{Q}$ is defined as

$$\vec{Q} = \left(\frac{2\pi}{\lambda}\right)\left(\vec{s} - \vec{s}_0\right) \tag{2}$$

where λ is the wavelength of the radiation, $\vec{s}_0$ and $\vec{s}$ are the unit vectors on the incident radiation direction and scattered radiation direction, respectively. The magnitude of $\vec{Q}$ is equal to $(4\pi/\lambda)\sin\theta$, where $2\theta = \theta_s$ is the scattering angle (the angle between incident ray and scattered ray). Therefore, very small scattering angles correspond to small values of the Q quantity. Analyzing Equation (1), we find that the intensity of the scattered radiation observed for a specific value of $\vec{Q}$ is equal to the square value of $A(\vec{Q})$, where $A(\vec{Q})$ is the suitable component of $\vec{Q}$ in the Fourier serial development of $\rho(\vec{x})$. For small values of $\vec{Q}$ that are produced at very small angles, the terms in $\rho(\vec{x})$ that define the quantity $A(\vec{Q})$ give a periodicity of $x = 2\pi/Q$, which is large enough in comparison with X-ray wavelength. These general considerations show that the very small diffraction angle (smaller than a few degrees) provides information on the structure of the matter to a relatively large scale in comparison with X-ray wavelength. It was experimentally observed that some samples generate a continuous and intense scattering at angles under 2°, without producing the normal diffraction effects from the usual X-ray experiments. This was first time noticed in specific types of fine carbon, black carbon powders, and different types of other substances, all having in common the fine particles of submicroscopic sizes. Later, it was concluded that continuous scattering around the direct beam is owed to the existence of the matter composed of small particles or, more general, to the existence of heterogeneities in the analyzed substance that can have dimensions from a few tens to a few hundred times the wavelength of the X-ray. The qualitative description of the central scattering, due to the presence of very small particles, could be done by analogy with the well-known light diffraction phenomena, which lead to the appearance of a halo when the light ray traverses a powder with grains having the dimensions 10 times larger than the wavelength of the light radiation.

http://dx.doi.org/10.5772/62184

Let us consider a particle bathed in an X-ray beam; thus all the electrons are wave scattering sources. If the scattering direction is the same as the incident ray, we can say that the scattered rays are all in phase and, if the scattering angle increases, the phase difference between the different scattered waves will also increase. Therefore, the amplitude of the resulting scattered wave will have values bigger or smaller in accordance only with the existing phase differences. This happens for a scattering angle about $2\theta = \lambda/D$, D being the average size of the particle, proving in this way that the study of central scattering offers a method to obtain the particle dimensions. This method is applicable only to the particles with dimensions between some specific limits. If D is too big, the scattering is limited to angles so small that are experimentally inaccessible. If D is too small, of the order of a few wavelengths, the scattering is too broad and too weak to be observed. To show more precisely which factors depend on the small angle scattering, let us consider a small particle of electronic density $\rho(\vec{x})$. Let us define a form factor $s(\vec{x})$ of this particle, which has a value of 1 when $\vec{x}$ vector is inside the particle, and a value of 0 when $\vec{x}$ is outside the particle. Thus, according to Equation (1), the amplitude of the scattered radiation from this particle will be

$$A_1\left(\vec{Q}\right) = \int \rho\left(\vec{x}\right) s\left(\vec{x}\right) \exp\left(-i\vec{Q}\cdot\vec{x}\right) d\vec{x} \tag{3}$$

If $A(\vec{Q})$ and $S(\vec{Q})$ are the Fourier transforms of $\rho(\vec{x})$ and $s(\vec{x})$, respectively, then

$$A_1\left(\vec{Q}\right) = A\left(\vec{Q}\right)\cdot S\left(\vec{Q}\right) \tag{4}$$

This can be demonstrated in the following manner. Let us consider the functions

$$a\left(\vec{x}\right) = \rho\left(\vec{x}\right) * s\left(\vec{x}\right) \text{ and } a\left(\vec{x}\right) = \int \rho\left(\vec{y}\right)\cdot s\left(\vec{x}-\vec{y}\right) dv_y$$

Thus, the Fourier transform of $a(\vec{x})$ is $A_1(\vec{Q})$;hence

$$A_1\left(\vec{Q}\right) = \int a\left(\vec{x}\right) \exp\left(2\pi i\vec{Q}\cdot\vec{x}\right) dv_x = \iint \rho\left(\vec{y}\right) s\left(\vec{x}-\vec{y}\right) \exp\left(2\pi i\vec{Q}\cdot\vec{x}\right) dv_x dv_y$$

Using the notations $Y = y$, $Z = x - y$

we replace the elementary differentials $dv_x dv_y$ with $dv_Y dv_Z$ and to obtain

$$\begin{aligned} A_1\left(\vec{Q}\right) &= \iint \rho\left(\vec{y}\right) s\left(\vec{Z}\right) \exp\left[2\pi i\vec{Q}\cdot\left(\vec{Y}+\vec{Z}\right)\right] dv_Y dv_Z = \\ &= \int \rho\left(\vec{Y}\right) \exp\left(2\pi i\vec{Q}\cdot\vec{Y}\right) dv_Y \cdot \int s\left(\vec{Z}\right) \exp\left(2\pi i\vec{Q}\cdot\vec{Z}\right) dv_Z = A\left(\vec{Q}\right)\cdot S\left(\vec{Q}\right) \\ A_1\left(\vec{Q}\right) &= A\left(\vec{Q}\right)\cdot S\left(\vec{Q}\right) \end{aligned}$$

Giving the dimensions of the region where $s(\vec{x})$ is different from zero, its transform $S(\vec{Q})$ is completely determinated and, if the particle has dimensions from some few tens to a few hundreds of atomic diameters, $S(\vec{Q})$ will be different from zero only for very small values of $\vec{Q}$. Now, let us consider the function $A(\vec{Q})$. If we suppose that the sample has a constant electronic density $\rho(\vec{x})=k$, then the transform $A(\vec{Q})$ will behave like a Dirac delta function, being zero overall with the exception of the point $\vec{Q}$ = 0, where it is infinite and $\int\delta(\vec{x})d\vec{x}=1$. We can conclude that small angle scattering is the method to study the dimensions of the system constituent particles, but the supposition of the existence of the identical particles separated by long distances between them is not quite accurate in the case of real samples. Therefore, the generalization of the theory is needed to take into consideration the diversity of particle sizes and shapes as well as the effect of particle close packing. Without considering the particles, a mathematical expression should be obtained for the scattered intensity in the vicinity of the center that should take into account the electronic density in all the points of the sample. Further, we will discuss only the process of single scattering, neglecting the multiple scattering phenomena and Compton scattering. We will consider an X-ray beam, sufficiently large to irradiate a large number of particles, but narrow enough in comparison with the sample-detector distance, to be like a ray in the experimental device geometry. The amplitude of scattered radiation from the P_n point (Fig. 2) will depend on the scattering factor u_n and the direction defined by the unit vector $\vec{s}$

$$A_n = A_e u_n \exp\left[-i\frac{2\pi}{\lambda}\left(\vec{s}-\vec{s}_0\right)\cdot\left(\overrightarrow{OP_n}\right)\right] \tag{5}$$

where A_e is the amplitude scattered by a single electron in the same conditions, O is an arbitrary origin that serves to describe the pathway difference between different rays, and $\vec{s}_0$ is the unit vector defining the incident radiation direction.

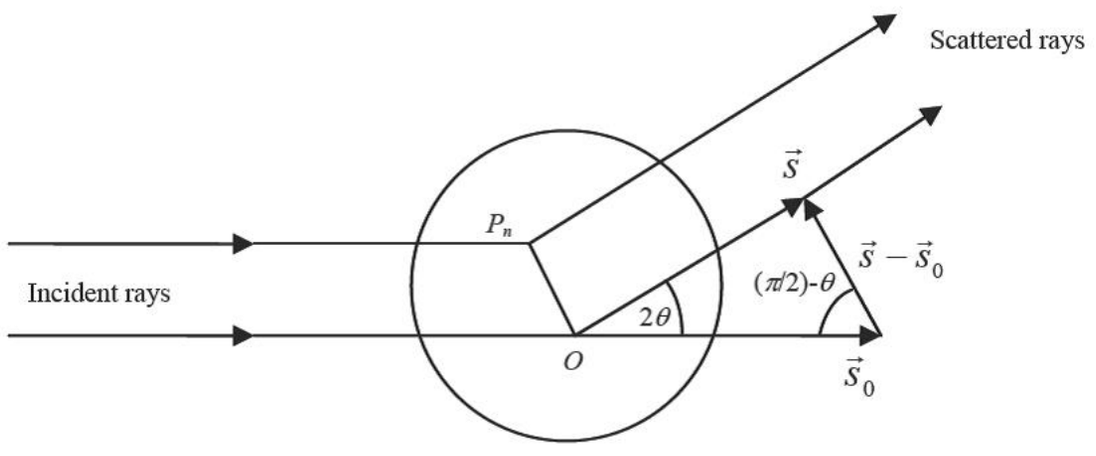

Figure 2. Diffraction by a scattering body.

The total amplitude of scattered radiation will then be

$$A\left(\vec{Q}\right)=\sum_{n}A_{n}=A_{e}\left(\vec{Q}\right)\sum_{n}u_{n}\exp\left(-i\vec{Q}\cdot\overrightarrow{OP_{n}}\right) \tag{6}$$

and the scattered intensity, the product between the amplitude A, and its complex conjugate A^{*}, will be

$$I\left(\vec{Q}\right)=\left|A_{e}(\vec{Q})\right|^{2}\sum_{n}\sum_{j}u_{n}u_{j}\exp\left[-i\vec{Q}\cdot\left(\overrightarrow{OP_{n}}-\overrightarrow{OP_{j}}\right)\right] \tag{7}$$

The intensity scattered by an electron is

$$I_{e}\left(Q\right)=A_{e}^{2}\left(Q\right)=A_{0}^{2}\frac{e^{4}}{m^{2}c^{4}}\cdot\frac{1}{r^{2}}\sin 2\theta=I_{0}\frac{e^{4}}{m^{2}c^{4}}\cdot\frac{1}{r^{2}}\sin 2\theta \tag{8}$$

which is a three-variable function, the incident intensity, the scattering angle, and the distance of observation; I_0 is the intensity of incident beam; and r is the distance from the particle to detector. If the analyzed environment has a center of symmetry, and this center is placed in the origin O, then to each $\overrightarrow{OP_n}$ vector will correspond another vector $-\overrightarrow{OP_n}$. Thus, we will obtain a simplified expression for the scattered amplitude:

$$A\left(\vec{Q}\right)=\sum_{n}A_{n}=A_{e}\left(\vec{Q}\right)\sum_{n}u_{n}\cos\left(\vec{Q}\cdot\overrightarrow{OP_{n}}\right) \tag{9}$$

We define the structure factor of the environment as the report between the total scattered amplitude and the radiation amplitude scattered by a single electron in the same conditions:

$$F\left(\vec{Q}\right)=\frac{\sum_{n}A_{n}(\vec{Q})}{A_{e}(\vec{Q})}=\sum_{n}u_{n}\cos\left(\vec{Q}\cdot\overrightarrow{OP_{n}}\right) \tag{10}$$

The scattered intensity will then be

$$I\left(\vec{Q}\right)=I_{e}\left(\vec{Q}\right)\left[\sum_{n}u_{n}\cos(\vec{Q}\cdot\overrightarrow{OP_{n}})\right]^{2}=I_{e}\left(\vec{Q}\right)F^{2}\left(\vec{Q}\right) \tag{11}$$

The term "P_n point" was used to define the structure of a particle. If we consider a large particle, the base element in its description is the atom; in this case, the point P_n refers to the center of the nth atom, and the scattering factor u_n is the scattering factor of this nth atom. In the interested angular domain for SAS, $u_n(\vec{Q})$ can be considered as a constant equal to $u_n(0)$. If we

consider a small region, then P_n point refers to a small volume element that surrounds it. The scattering factor u_n is then equal to $\rho_n dv_n$, where ρ_n is the electronic density of the particle in the vicinity of P_n point, and dv_n is the volume of considered element. Generally, it is convenient to describe the particle structure taking into account enough small elements to consider the scattering factors of these elements to be constant, independent of scattering angle over the whole domain where the structure factor of the considered particle is different from zero. This theory of small angle X-ray scattering can be adapted very easily to neutrons.

Small angle neutron scattering is used where the X-rays cannot provide the desired information either of the lack of scattering contrast or of severe absorption of the studied material. The choice of thermal neutrons as a means of substance investigation was owed to their wavelengths and their energies corresponding to the inter atomic distances and excitation energies of condensed matter. Neutron absorption from the matter is very low, thus resulting in the samples that can have thicknesses larger than in the X-rays case which are strongly absorbed with an increase in the volume of analyzed samples. We can say that SANS allows the investigation of materials in various conditions, such as in containers, furnaces, cryostats, etc. Due to its magnetic moment, the neutron provides unique possibilities to the study of magnetic structures, magnetic moment distribution, and magnetic excitations. Being a nuclear propriety, the nuclear scattering amplitude can be considerably different between various isotopes of a specific chemical species. For example, the big difference between the coherent scattering lengths of hydrogen and deuterium lead to the usage of phase contrast in the study of hydrogenate materials, allowing a good resolution in analyzing polymers and biological substances in general. Because thermal neutrons interact very low with the matter, this interaction can be theoretically treated on the base of first Born approximation [5, 6]. We will show further that the variation of the scattering density is very important in the study of condensed matter through SANS. In the following, we will consider the "static approximation"; the scattering process is produced only at nuclear level on fixed targets letting those targets unchanged after the collision, and without considering the polarization effects.

Thus, we can write the coherent elastic scattering differential cross section on a single atom:

$$\frac{d\sigma}{d\Omega} = \frac{1}{N}\left|\sum_R b_R \exp\left(i\vec{Q}\cdot\vec{R}\right)\right|^2 \tag{12}$$

where N is the number of scattering nuclei exposed to the beam, and b_R is the coherent scattering length of the chemical species that occupy a specific place determined by the position vector $\vec{R}$. If we replace b_R through an average local scattering length density $\rho_b(\vec{r})$, where $\vec{r}$ is a continuously variable position vector, we can write

$$\frac{d\sigma}{d\Omega} = \frac{1}{N}\left|\int_V \rho_b\left(\vec{r}\right)\exp\left(i\vec{Q}\cdot\vec{r}\right)d^3\vec{r}\right|^2 \tag{13}$$

http://dx.doi.org/10.5772/62184

where the integration is performed over the whole sample volume V.

The scattering length density $\rho_b(\vec{r})$ can now vary on distances of the order of d_{min}, where $d_{min} \cong \pi/Q_{max}$, Q_{max} being the maximal value accessible by experiment. Thus, we can write that

$$\rho_b(\vec{r}) = \Delta\rho_b(\vec{r}) + \vec{\rho}_b \tag{14}$$

where ρ_b is averaged on volumes larger than the instrument resolution volume, determined by the minimum observed value of Q. Therefore, the cross section that contains the useful information about the studied system is dependent on $\Delta\rho_b(\vec{r})$. By substituting Equation (14) in Equation (13) we obtain

$$\frac{d\sigma}{d\Omega} = \frac{1}{N}\left|\int_V \left[\rho_b(\vec{r}) - \overline{\rho_b}\right]\exp\left(i\vec{Q}\cdot\vec{r}\right)d^3\vec{r}\right|^2 \tag{15}$$

For a specific distribution of scattering length, the cross section can be analytically calculated with the help of Equations (13) and (15). Because the cross section values are not known everywhere in reciprocal space, $\rho_b(\vec{r})$ determination by experimental measurements of $d\Sigma/d\Omega$ values is very hard to be carried out, or even impossible. Let us take a sample containing N_p particles with scattering length densities $\rho_{bp} = b_p/v_{ap}$, where b_p is the scattering length averaged on the particle volume, and v_{ap} is the atomic volume from the particle. Let us consider that these particles are packed in a homogeneous matrix having scattering length densities $\rho_{bm} = b_m/v_{am}$.

Using Equation (13) we obtain

$$\frac{d\Sigma}{d\Omega}\left(\vec{Q}\right) = \frac{1}{N}\left(\rho_{bp} - \rho_{bm}\right)^2\left|\int_{V_t}\exp\left(i\vec{Q}\cdot\vec{r}\right)d^3\vec{r}\right|^2 \tag{16}$$

where the integral is extended over the volume V_t occupied by all the particles. In the most general case, this integral will contain spatial and orientation correlation elements between particles, and effects owed to the size distribution of the particles. Taking into account the form factor expression for a single particle

$$F_p\left(\vec{Q}\right) = \frac{1}{V_p}\int_{V_p}\exp\left(i\vec{Q}\cdot\vec{r}\right)d^3\vec{r} \tag{17}$$

where V_p is the particle volume so that $|F_p(0)|^2 = 1$. We will now consider N_p identical particles for which we can write the following expression

$$\frac{d\Sigma}{d\Omega}\left(\vec{Q}\right) = \frac{V_p^2 N_p}{N}\left(\rho_{bp} - \rho_{bm}\right)^2\left|F_p\left(\vec{Q}\right)\right|^2 \tag{18}$$

that is valid in the case of binary systems, without contributions from the interferences between particles.

The interference term from Equation (16) that was neglected in Equation (18) is the Fourier transform $\Psi(\vec{Q})$ of the correlation function:

$$\Psi\left(\vec{Q}\right)=\frac{1}{N_p}\sum_{i\neq j}\exp\left[i\vec{Q}\cdot(\vec{r}_{0i}-\vec{r}_{0j})\right] \tag{19}$$

where $\vec{r}_{0i}$ and $\vec{r}_{0j}$ are the position vectors of the particle centers denoted by *i* and *j*.

The $\Psi(\vec{Q})$ function will be zero for all the values of $\vec{Q}\neq 0$ if the distance distribution between the particles is completely random, approximately like in the case of very diluted systems. Equation (18) is valid for particles anisotropically oriented, but all are identically oriented. In most cases of random distribution of the orientations or in discrete but multiple orientations of anisotropic particles, suitable averages of $|F_p(\vec{Q})|^2$ are used. Guinier shows that at small values of *Q*, the scattering function $S(\vec{Q})=|F(\vec{Q})|^2$ for a specific physical system can be written as

$$S\left(\vec{Q}\right)=\exp\left(-Q^2R_D^2\right) \tag{20}$$

where R_D means the gyration radius which is a material parameter having the length dimension defined through

$$R_D^2=\frac{1}{V_p}\int_{V_p}r_D^2q\left(r_D\right)dr_D \tag{21}$$

where $q(r_D)$ is the geometrical cross section of the particle, through the length of a plane normal to a direction *D* and at a distance r_D from the origin inside the particle. For a system of particles randomly oriented

$$S\left(\vec{Q}\right)=\exp\left(-Q^2R_G^2/3\right) \tag{22}$$

with

$$R_G^2=\frac{1}{V_p}\int_{V_p}r^2d^3\vec{r} \tag{23}$$

http://dx.doi.org/10.5772/62184

For spheres of radius R_S, $R_G = (3/5)^{1/2}R_S$, and Equation (21) coincides with the expression

$$S_S\left(QR_S\right) = \left[3\left(\sin\left(QR_S\right) - QR_S\cos\left(QR_S\right)/Q^3R_S{}^3\right)\right]^2$$

to the term proportional with Q^4. The subsequent terms in the developments of the two series are in a good concordance, but the corresponding terms have the same sign. Guinier approximation is thus accepted over a large range of QR_G(<1.2).

For rotational ellipsoids, the Guinier approximation coincides with the extension of scattering functions until Q^6. For other shapes of the particles, it might be necessary for an investigation of the small values of Q to be able to determine R_G with sufficient accuracy. In the case of homogeneous particles, with pronounced margins and area A_p, Porod has proved that

$$\overline{S\left(\vec{Q}\right)} \cong 2\pi A_p / V_p^2 Q^4 \tag{24}$$

This shows the average decrease in the scattering function at large Q. Q should be larger than the reciprocal value of the smallest dimension of the particle.

3. Experimental methods used in the study of condensed matter by SANS

The goal of SANS method is to measure $I(Q)$ and to extract from that measurement the "structural" data regarding the studied system. The quantity Q is defined as $Q = \frac{4\pi\sin\theta_s}{\lambda} \approx \frac{2\pi}{\lambda}\theta$, if $\theta = \frac{\theta_s}{2}$ is small enough.

Therefore, to measure $I(Q)$, it is sufficient to measure $I(\theta)$ at constant λ or $I(\lambda)$ at constant θ. In the following, we will discuss both experimental alternatives.

3.1. The method $I(\theta)$ at constant λ

This method is based on monochromatic (λ = constant) beam extraction from the white thermal neutron spectrum provided by a research reactor. The thermal neutrons released from the reactor are first collimated with a Soller collimator (with plane parallel slits) and after that they are monochromatized with either a mechanical monochromator or a crystal. Monochromatization is the method that allows the extraction of desired neutrons from the neutron beam provided by the source; in other words, to obtain thermal neutrons with energies in a very narrow interval centered around a value E_0 of the energy. Neutron monochromation is based either on their corpuscular proprieties (mechanical monochromators) or on their wave proprieties (crystal monochromator). The mechanical monochromator is a cylinder endowed with helicoidal slits on the whole length of its generatrix.

When the cylinder is rotating with the angular speed ω, the neutrons with their motion direction parallel with the rotor axis would traverse the monochromator slits without modifying their distance to the slits walls only if they would have a specific speed v_0, directly correlated with ω and which is corresponding to the wavelength λ_0 of the neutrons transmitted by the monochromator. Another type of mechanical monochromator uses disks instead of a cylinder. Its functional principle is identical with the cylindrical monochromator, but having the difference that the place of helicoidal slits is taken by straight slits cut off on a rigid mounted disc on a horizontal axis, which rotates with an angular speed ω. The disks are positioned on the axis having the slits displaced to provide a selective opening in accordance with the axis rotation speed ω, only to the neutrons moving with a specific speed v_0. Nevertheless, the most used monochromatization method is by using a crystal. Crystal utilization in spectrometer devices is based on the neutron diffraction phenomena.

Monochromatic neutron beam separation from the thermal neutron beam provided by the reactor is realized through its Bragg reflection on a monocrystal. If we note the distance between the crystalline planes with d_{hkl} determined by the h, k, l indexes, and θ_B the neutron incident angle on these planes, then the reflected neutron wavelength is given by the Bragg law

$$n\lambda = 2d_{hkl}\sin\theta_B = \frac{nh}{\sqrt{2mE}}$$

where m and E are the neutron mass and neutron energy, respectively, but n is the reflection order.

In other words, if a monocrystal is used to select neutrons with a specific wavelength λ that satisfies the Bragg relation, then the neutrons selected by the crystal would also have the wavelengths $\lambda/2$, $\lambda/3$, $\lambda/4$,..... etc., which means that reflections with a higher order take place, with n = 1, 2, 3,.... In the case of monochromators with crystal, the presence of high-order reflections could be a serious problem because sometimes, depending on the spectral distribution of the incident beam and the crystal structure factor, the reflection intensities become comparable and even greater than the first-order reflection intensity. In most neutron physics experiments, first-order reflection (n = 1) is used, but other reflections (high-order contaminations) should be eliminated by different means.

Analyzing the Bragg relation, we can see that by using of monochromator crystals, only monochromatic neutrons with the wavelength of $\lambda_{max} \leq 2d_{max}$ can be selected, where d_{max} is the maximum distance between the crystal planes. The neutrons having the wavelength $\lambda > 2d_{max}$ are not presenting Bragg reflections.

This observation suggests a simple way to eliminate the second-order reflections, utilized mostly when the monochromatic neutrons desired to be extracted from the reactor emergent beam have wavelengths relatively large, for example, in the range $\lambda > 6$ Å. It is sufficient to introduce a polycrystalline filter of convenient size in the pathway of neutron beam falling on the monochromator crystal, with its crystalline structure characterized by $d_{max} < \lambda_0/2$, where λ_0

http://dx.doi.org/10.5772/62184

is the wavelength of the neutrons to be extracted. There is another experimental solution to eliminate second-order reflections, for example, using a monochromator of special monocrystals with an internal composition that cancels the structural factor for some specific groups of crystalline indexes. Because the problem of high-order reflections is overpassing the goal of this chapter, we will not insist on this subject.

Frequently, the experimental pattern used to obtain monochromatic neutron beams in this way contains a Soller collimator which spatially delimitates the incident neutron beam coming out from the reactor, the monochromator crystal, and the second Soller collimator which delimitates the diffracted beam. Simultaneous rotations of the second collimator and the crystal with angular speeds staying in a ratio of 2:1 allows to extract monochromatic neutron beams of different wavelengths from the continuous spectrum of the incident thermal neutron beam. The monochromatic neutrons are recorded by a detector placed after the second collimator rotating in the same time with it.

The devices built on this principle, the so-called neutron spectrometer with crystal, allow the determination of total cross section by the measurement of sample transmission in accordance with neutron wavelength. To study the angular distribution of scattered neutrons by a certain target and implicitly to measure the differential cross sections, a pattern with a third Soller collimator between the sample and detector is used. To investigate the neutron scattering of different wavelengths, the whole system built from the second collimator, the studied sample, the third collimator, and the neutron detector should be rotated around the first fixed axis that is going through the middle of the monochromator crystal and together with it; the angular speed ratio of the crystal and the mentioned system should be 1/2. For a certain position of the monochromator crystal and the second collimator, the third collimator and the detector could be rotated around the second fixed axis (that is going through the middle of the sample) allowing the measurement of sample differential cross section for thermal neutrons having the wavelengths determined by the monochromator preceding the sample. This experimental pattern is named neutron spectrometer with two axes. Many experimental systems use optical patterns derived from the two axis spectrometer described earlier. Anticipating the discussion in the next section, we would mention that from the simple presentation of the optical pattern of considered spectrometer arises a specific limitation of its efficiency. Actually, to measure $I(Q)$ with sufficient precision in the optical pattern described before, it is necessary to increase the distances (R) between the studied sample and the detector, as much as possible; increasing this distance obviously will lead to decreasing the lower limit of the explored Q range. Because the intensity of the scattered beam varies with $1/R^2$, the obtained resolution gain is drastically affected by losing the luminosity of the experimental system. If we add to this inconvenience the construction of experimental devices having excessive dimensions, the continuous search for more efficient SANS optical patterns becomes explicable. One of the identified optical patterns which is considered most acceptable is by using two crystals, with the sample staying between them.

Two crystal systems were used as monochromators in spectrometric assemblies long time ago, first in X-ray physics and then in neutron physics. To discuss the utilization manner of two monocrystals systems in SANS, we have to reveal the optical characteristics of these systems.

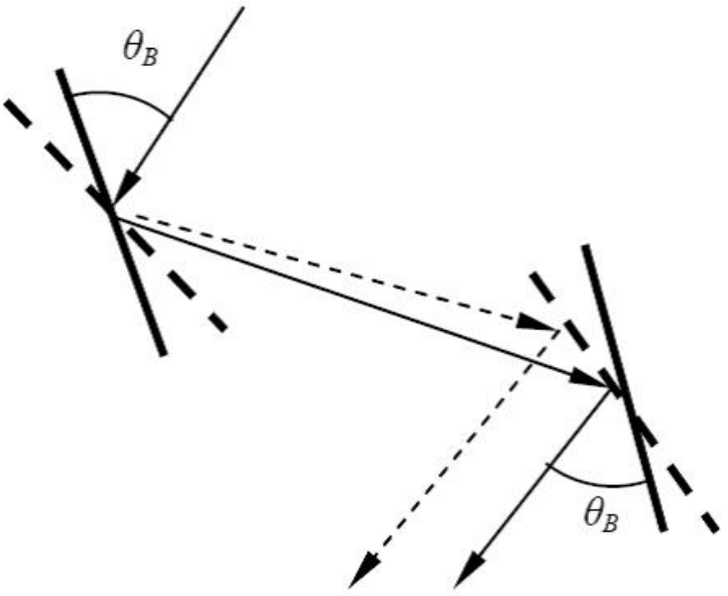

Figure 3. Parallel pattern.

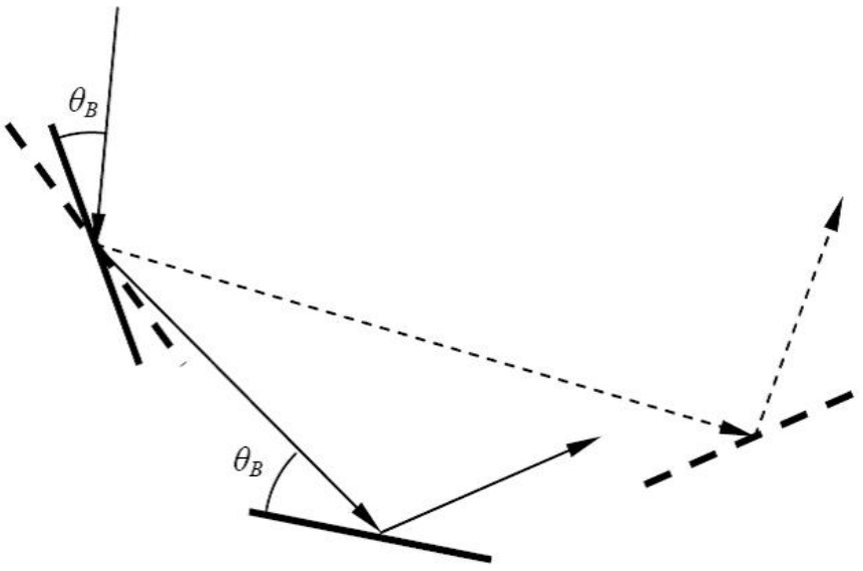

Figure 4. Antiparallel pattern.

To simplify the explanation, we will limit our case to consider that the two monocrystals are ideal identical crystals, from the point of view of their internal crystalline structure and their cutting method (has the same active reflecting planes). A two-monocrystal system could work in two optical patterns: parallel (Fig. 3) and antiparallel (Fig. 4).

In the parallel pattern, any selected wavelength from the incident polychromatic beam through Bragg reflection on the first crystal leads to the propagation of the double reflected beam in parallel direction with the incident beam. Therefore, this pattern is not dispersive (does not

http://dx.doi.org/10.5772/62184

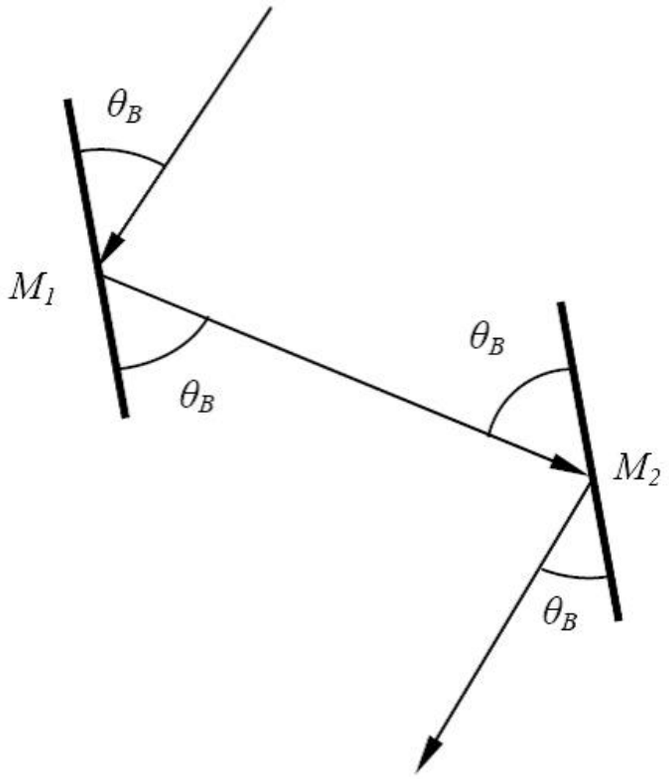

Figure 5. Double crystal parallel pattern.

spatially separate the beams of different wavelengths). In the second optical pattern, the Bragg double reflected beam is propagated on a direction oriented toward the region containing the radiation source and is named antiparallel. To notice that the wavelength change of the selected radiation beam through double reflection is realized along two directions depending on the wavelengths, revealing the dispersive feature of the antiparallel pattern. In the case of the parallel pattern, the thermal neutron beam falling on the first monochromator crystal under the incident angle θ_B, it will be Bragg reflected on the second crystal, the double reflected ray making the same angle θ_B with the second crystal (Fig. 5).

If a sample is interposed between the two crystals, then the beam reflected by the first crystal will be scattered by the sample under the θ_S angle and will fall on the second crystal under the θ incident angle (Fig. 6).

To detect the scattered beam, we have to rotate the second monochromator crystal together with the detector by an angle α; thus the Bragg relation is satisfied by obtaining the same incident θ_B angle for the sample scattered ray. Among these angles, we can write the following relations:

$$\theta - \alpha = \theta_B \Rightarrow \theta - \alpha = \theta_B$$
$$\theta_S + \theta_B = \theta \Rightarrow \theta - \theta_S = \theta_B \Rightarrow \alpha = \theta_S$$

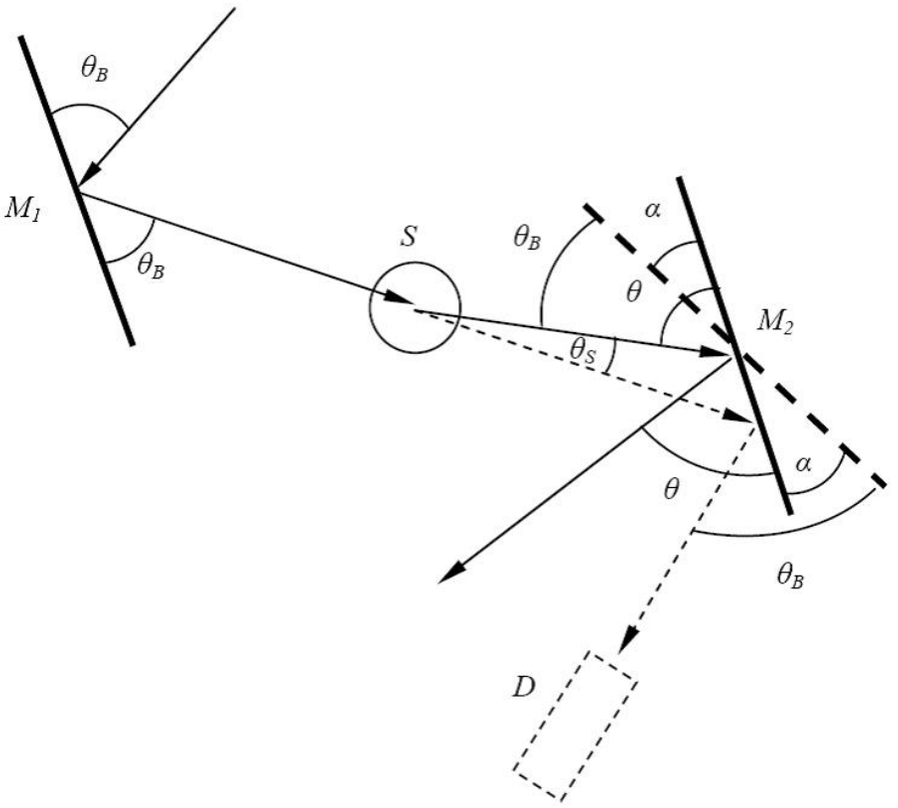

Figure 6. Three axes parallel pattern.

Because the sample is scattering, the neutrons under different angles $\theta_S(\theta_{S1}, \theta_{S2},..., \theta_{Sn})$ arise that the system composed from the second monochromator and the detector should be rotated in accordance with the suitable $\alpha(\alpha_1, \alpha_2,..., \alpha_n)$ angles to be able to detect all scattered neutrons. Let us now consider the case of the antiparallel pattern. The thermal neutron beam falls on the first monochromator crystal under the incident θ_B angle and is reflected on the second monochromator crystal, the double reflected ray leaving the system under the same θ_B angle (Fig. 7).

If we have a sample between the two crystals, then the reflected beam by the first crystal will be scattered by the sample under a θ_S angle and will fall on the second crystal under the θ angle (Fig. 8).

The neutrons scattered by the sample S could be detected only by rotating the second crystal with the α angle, thereby reestablishing the Bragg law by remaking the initial incident θ_B angle. Also, we found that

$$\theta + \alpha = \theta_B \Rightarrow \theta + \alpha = \theta_B$$
$$\theta_B - \theta_S = \theta \Rightarrow \theta + \theta_S = \theta_B \Rightarrow \alpha = \theta_S$$

http://dx.doi.org/10.5772/62184

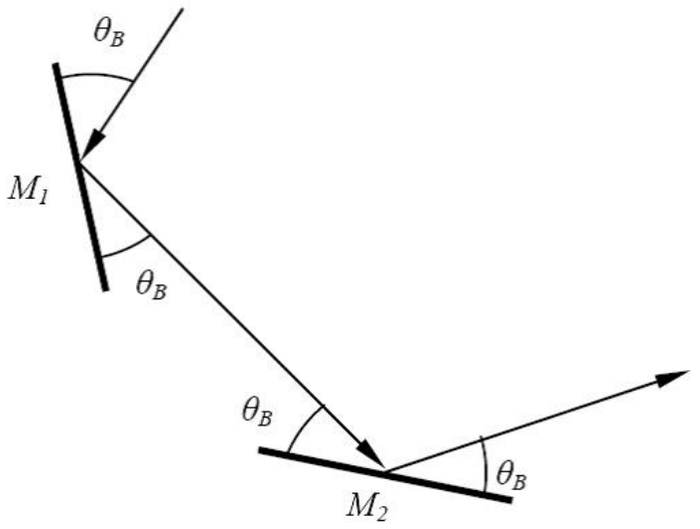

Figure 7. Double crystal antiparallel pattern.

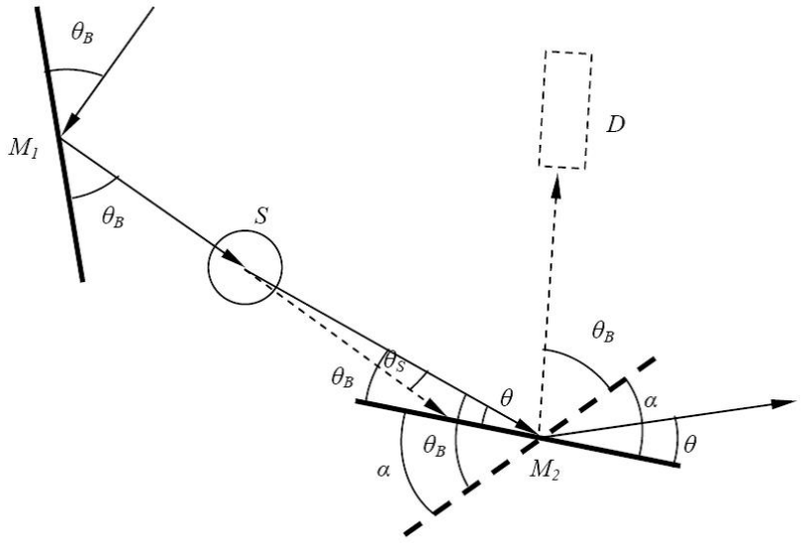

Figure 8. Three-axe antiparallel pattern.

To notice that this pattern is the most frequently used due to its dispersive feature this allows a better measurement of the interest neutrons.

3.2. The method $I(\lambda)$ at constant θ

Another method is to make the observation only on a certain scattering direction 2θ = constant. This time the directly measurable quantity is the wavelength (or the energy) of the coherent radiation scattered by the sample. This method is based on λ determination for every detected neutron, by its time of flight measurement along a known distance. According to the De Broglie equation

$$\lambda = \frac{h}{mv} = \frac{ht}{mL}$$

where L is the distance between the neutron source and detector, h is the Planck constant, and m is the neutron mass. The neutrons with a wavelength λ will have a speed $v = h/m\lambda$ so that to cover an L distance, the time $t = L/v$ will be necessary.

Neutrons of different wavelengths will need different time to cover the same distance L. If the moment of neutron pulse emission coincides with the time scale origin of the neutron detector impulse analyzer, the detector impulse selection in accordance with the impulse appearance time (practically by neutron arrival time) allows the spectral distribution measurement of the neutron beam. The electronic devices performing this selection are "the time of flight analyzers." The analyzer has a number of channels in which the impulses are accumulated due to the neutrons arriving to the detector in the time intervals $t_0 + \tau$, $t_0 + 2\tau$, $t_0 + 3\tau$, and so on.

Here, t_0 represents a "delay time" of the impulse temporally analyzer system start-up, which could be varied with the used experimental pattern particularities, and τ is the channel temporal width, a quantity that can be varied in stages for a specific instrument. The measurements by the time of flight method can be made using both steady-state reactors and pulsed reactors as neutron sources.

In the case of steady-state reactors, the neutron beam leaving the reactor channel meets an obturator in its way which opens the way only for very short time intervals. In this manner, the detector "notices" a pulsed neutron beam with a determined time length, for a specific obturator–detector distance, by the neutron energetic spectrum. The detector is connected with a time of flight analyzer, which can be unleashed by the obturator opening. To the pulsed reactors, the obturator function is undertaken by the neutron source itself. The time of flight analyzer start-up command is given by the neutron source when the pulse is accomplished. In every SANS experiment, the main goal is to determine with a good precision and in a reasonably short time the Q dependence of the analyzed sample coherent elastic scattering differential cross section in a large as possible Q variation range. From the point of view of the Q range explored value extension, the two SANS investigation methods indicate the following possible performances:

$$\frac{Q_{\max}}{Q_{\min}} = \left[\frac{\theta_{\max}}{\theta_{\min}}\right]_{\lambda=\text{const.}} \quad \text{and respective} \quad \frac{Q_{\max}}{Q_{\min}} = \left[\frac{\lambda_{\min}}{\lambda_{\max}}\right]_{\theta=\text{const.}}$$

For any $Q_{\max} - Q_{\min}$, the interest interval for a certain sample, the first method seems to be more reasonable because the Q limitation apparently is dictated only by the measurement conditions, but in the case of the second method, the λ limitation is dictated by the spectral characteristics of the neutron source. If the neutron source is in steady state, then the first method utilization is certainly more advantageous because pulsing the neutron beam with a chopper leads to a usage of 10^{-4}–10^{-3} from the produced neutrons even if we consider the advantage of

http://dx.doi.org/10.5772/62184

the second method to replace the sequential measurement of $I(Q)$ with the simultaneous one. The advantage of the first method toward the second in the case of utilization of a steady-state source is more evident if we estimate the consequences resulting in the obtained precisions and the experiment duration from the efficient utilization of the neutron beam emitted by the source. In the case of pulsed sources, the same criteria of neutron beam efficient utilization impose the application of the second working method. The approximate equivalence of the two methods, the first by the steady-state reactors and the second the pulsed sources, can be motivated that in present, at realized impulse fluxes and obtained pulses frequencies, the pulsed sources lead to getting middle fluxes comparable with the one obtained from the steady-state reactors of the same category. All these reasons justify the topics discussed in the next section, the presentation of SANS equipment used by the first method at the steady-state reactors or the second method used at the pulsed sources.

4. Experimental patterns

4.1. The method $I(Q)$ at constant λ

As it was discussed in Section 3, from among the optical patterns, the one with two crystals and the sample situated between them is much more appreciated. This pattern was used in many reactors, and a typical description of it is given in Fig. 9.

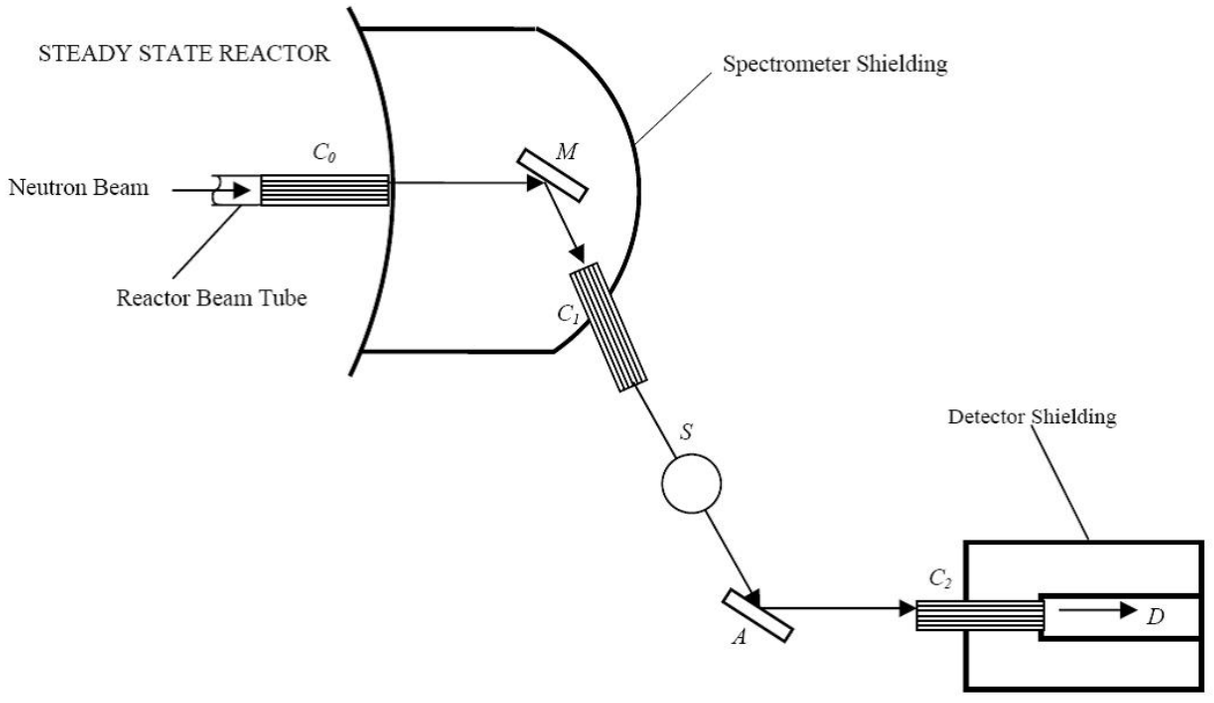

Figure 9. Three-axe spectrometer.

The monochromator group built by C_0 and C_1 collimators, and the monocrystal M sets up a monochromatic beam falling on the studied sample S. The analyzing group formed by the monocrystal A, the collimator C_2, and the detector D is initially tuned to detect the incident neutrons in the sample. To determine the neutron angular distribution produced by small angle scattering in the sample, we have to perform a combined scanning of the detector and the analyzer crystal around a vertical axis going through the center of the A crystal. Let us consider a small reactor providing a neutron flux of 1×10^{13} neutrons/cm^{2}s at 2 MW maximal power. From the white thermal neutron flux transmitted through the C_0 collimator, the M monochromator selects a very narrow band centered around the $\lambda = 1.15$ Å, with a wavelength resolution of $\Delta\lambda/\lambda = 4.5 \times 10^{-3}$. This beam is transmitted further through the C_1 collimator to the analyzed S sample and scattered at small angles (between 0 and 2 minutes). The A crystal collects the scattered beam and transmits it to the D detector through the C_2 collimator.

We consider that both crystals are copper monocrystals identically cut, with the reflecting plane orientation in the (002) direction and a mosaic divergence structure of 14 minutes. The C_0 and C_1 collimators have an angular horizontal divergence of 10 minutes, while that of the C_2 collimator is only of 5 minutes. The 2θ monochromator angular range is 50° but the scattering range of monochromator and analyzer is maximum 120°. The detection system is an ordinary BF_3 detector. Another type of neutron spectrometer is by using a cold source to allow neutron moderation at low temperatures, such as the VVR-SM reactor from Budapest Neutron Center (BNC). With an active core providing an average power of 10 MW, the neutron balance is improved by the mean of a beryllium reflector up to 10^{14} neutrons/cm^{2}s. The small angle scattering spectrometer described (Fig. 10) in the following is a conventional one. It uses a mechanical monochromator instead of a crystal monochromator. The mechanical selector with helical slits gives a wavelength resolution $\Delta\lambda/\lambda$ between 5 and 20% for a λ lying between 3.5 and 8 Å.

The neutron beam is geometrically built up by a 3 m-long vacuum collimator. The maximal beam dimension in the sample is 2 cm diameter. The distance from the sample to detector can vary from 1 to 5 m. The spectrometer is provided with an automatic sample changer controlled by a computer. The scattering vector range lies between 5×10^{-3} Å$^{-1} < Q < 2$ Å^{-1}. The scattered neutrons are detected by an XY positional detector with BF_3 having the dimension 64×64 cm^2.

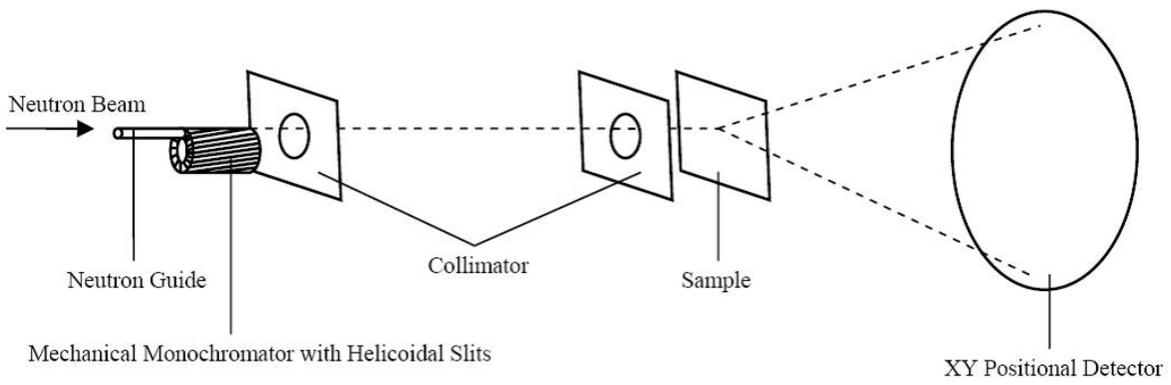

Figure 10. Spectrometer with mechanical monochromator.

http://dx.doi.org/10.5772/62184

Measurement instrument control and experimental data collection are performed by a computer.

4.2. The method $I(\lambda)$ at constant θ

This method is used mostly for the neutron pulsed sources. This type of spectrometer built on the time of flight principle is installed to the IBR-2 pulsed nuclear reactor at Joint Institute for Nuclear Research (JINR) in Dubna, Russian Federation. The name of the spectrometer is YuMo [7], given from its constructor, the scientist Yu. M. Ostanevich (Fig. 11). The reactor fuel is plutonium oxide, and uses liquid sodium as a coolant. The reactor reflector is composed of a static part and a rotational one with constructive and movement characteristics that determine the issue of fast neutron pulsed flux. The produced neutrons are moderated in water and through the horizontal beam tubes that surround the reactor active core in the experimental hall.

In the current working conditions, the reactor provides a maximum flux of thermal neutrons of 10^{16} neutrons/cm^{2}s per pulse at the moderator surface. The frequency of pulse repetition is 5 Hz.

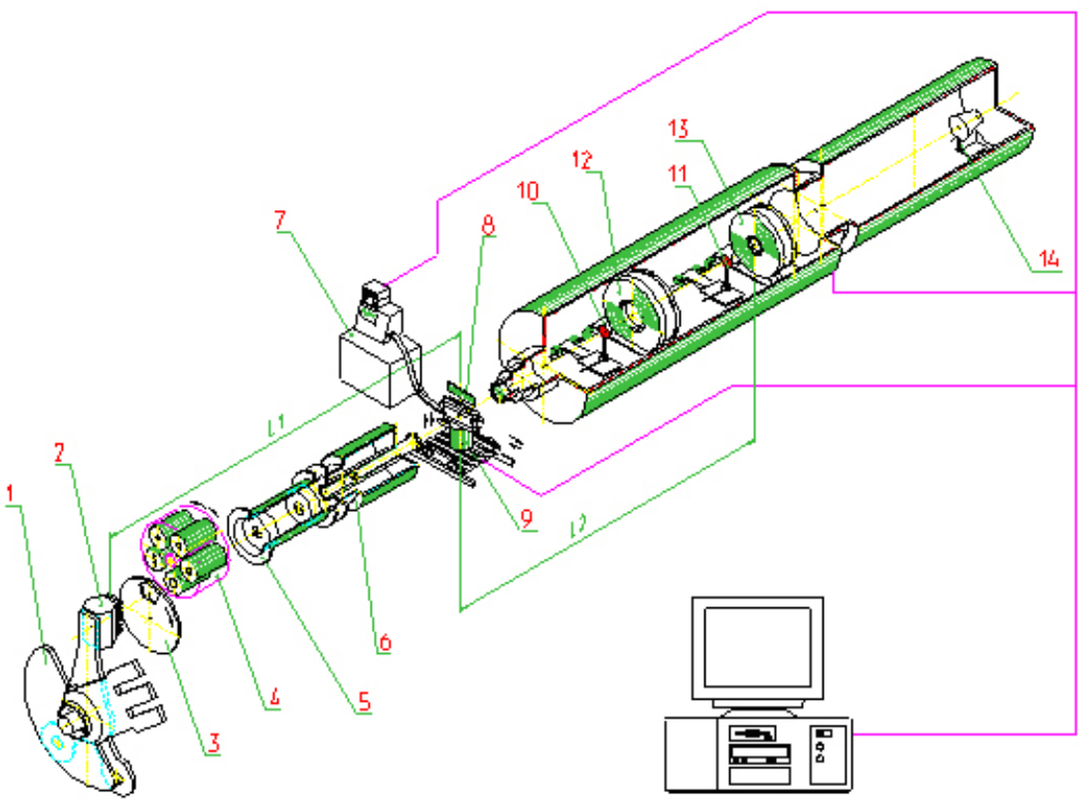

Figure 11. SANS spectrometer YuMo.1) two reflectors, 2) zone of reactor with moderator, 3) chopper, 4) first collimator (C1), 5) vacuum tube, 6) second collimator (C2), 7) thermostat, 8) samples table, 9) goniometer, 10)–11) vanadium standard, 12) ring-wire detector, 13) position-sensitive detector "Volga," 14) direct beam detector.

The chopper placed after the neutron moderator plays the main role to remove the neutrons from other reactor pulses and to assure that the neutrons from the interested pulse arrive at the detector. The neutron tube is made by steel pipes of different diameters and is kept under vacuum of about 10^{-2} Torr to avoid neutron absorption.

It is connected to the central vacuum system which is controlled from reactor control room and is provided with a mechanical beam stop that automatically closes the beam. A complete cycle of closing–opening the beam stop lasts about 6 minutes. The chopper is followed by a collimator with discrete variable aperture (C_1) that assures a geometrical pre-shape of the neutron beam and by the monitor whose signals are used for the normalization of the data obtained from different reactor pulses. The next collimator (C_2) assures the geometrical profile of the incident neutron beam in the sample and defines its dimensions. The collimator (C_1) is composed of four cylinders of different diameters (100 mm, 80 mm, 60 mm, and 40 mm), but with the same length which can be remote-controlled to be aligned in the neutron beam by a rotational movement in accordance with the experimental requirements of the beam geometrical pre-shape. The collimator (C_2) which limits the geometrical profile of the incident neutron beam in the sample has a remote-controlled variable opening (28 mm, 14 mm, and 7 mm). The holder with the collimation orifices of the (C_2) collimator are made from boron polyethylene having an insignificant scattering cross section in comparison with the absorption cross section. All collimators and the most important shielding elements are covered with a mixture of polyester and boron carbonate or boron acid. The sample holder having six slots is connected to a special remote-controlled mechanism of sample changing that allows each sample to be introduced in the neutron beam according to the experimental program. The sample is placed at 18.74 m from the moderator surface. The sample holder is provided with a cooling and warming system that allows adjusting the sample temperature between 20 to 150°C.

To record and analyze the scattered neutrons in accordance with their time of flight, the experimental equipment is provided with a measurement system having two detectors. The detectors are functionally identical but different by dimensions that assure their efficiency in observing the Q values at small and large ranges. Therefore, both detectors are provided with eight active ring detectors; one detector having the central opening of 80 mm while the second of 200 mm having outside diameters of 730 mm and 560 mm, respectively. Each detector can be settled in one of the eight positions having the sample detector distance fixed in the interval of 4.5 –12.5 m. The active part of each detector is divided into eight independent ring detectors by means of a concentric copper partition (the cathodes); at the center of each ring exists a tungsten wire of 25 μm thickness (the anode). This type of assembly provides eight independent ring detectors that offer more accuracy of the measurements by partial overlapping of the detection range of each ring with the range of the previous ring. The detector efficiency for neutrons with λ = 1.8Å is about 70%.

The detector room is located after the samples and is made from a steel pipe of 1200 mm diameter and 12 m length having the inside surface covered with a cadmium layer of 0.5 mm thickness. Inside the room are mounted two rails for the movement of the electric-driven detectors trucks. The incident neutron beam is transmitted through the central hole of the detectors. At a distance of about 1.5 m from the reactor side, the detector is placed on a truck-

http://dx.doi.org/10.5772/62184

driven mechanism in the vanadium standard (a vanadium metal sheet of about 0.3 mm thickness) that allows the introduction of the beam according to a program. This standard is used for the obtained experimental data calibration. The incident beam detector placed after the annular detectors measures the spectral distribution of the incident neutrons in the sample and forwards the normalization to this spectra of the scattered neutron spectra.

5. Conclusions

To summarize, we can say that small angle scattering is the collective name given to the techniques of SANS and SAXS scattering. In each of these techniques, radiation is elastically scattered by a sample, and the resulting scattering pattern is analyzed to provide information on the size, shape, and orientation of some components of the sample. They offer the possibility to analyze particles without disturbing their natural environment. The type of sample that can be studied by SAS, the sample environment that can be applied, the actual length scales that can be probed, and the information that can ultimately be obtained all depend on the nature of the radiation used. For example, SAXS cannot be used to study thick samples or samples requiring complex containers, while SANS can penetrate deeper in the condensed matter. SANS is produced by heterogeneities in matter. If these are randomly oriented, every atom pair contributes to the scattering of a sample. Inhomogeneities of sizes larger than atomic distances (10–1000 Å) produce scattering patterns with Q ranges $1/D < Q < 10/D$, if D is the dimension of the inhomogeneities.

A scattering experiment sees a scattering length density; in the case of X-rays, this is simply the electron density. The absolute density is not important but, in contrast, the difference between the particle and the surrounding medium.

The result of the experiment is the Fourier transformation of the contrast distribution. By comparing the experimental data with the theoretically calculated intensities or by a Fourier back transformation, we receive information about the contrast distribution, e.g., the mass density distribution of one particle. In the case of concentrated systems, we receive combined information about the single particle and the interaction between different particles.

In most cases, the sample and/or the sample environment are rather bulky.

Therefore, SANS instruments usually have to be large themselves in order to yield the desired resolution. Small SANS instruments can only serve a very limited number of applications. For reasons of intensity, a relatively large beam divergence, i.e., a beam cross section larger than the sample size is accepted as well as wavelength resolutions $\Delta\lambda/\lambda$ of up to about 20%.

SANS and SAXS techniques are complementary; however, they share several similarities. Perhaps the most important of these is the fact that, with minor adjustments to account for the different types of radiation, the same basic equations and "laws" (for example, those due to Guinier and Porod) can be used to analyze data from any of the two techniques. This is a great advantage and one that has certainly eased the transition from one technique to another.

Author details

Cristian A. Dragolici*

Address all correspondence to: adrag@nipne.ro

Horia Hulubei National Institute for R&D in Physics and Nuclear Engineering (IFIN-HH), Bucharest-Magurele, Romania

References

[1] Guinier A., Fournet G. Small-Angle Scattering of X-rays. New York: John Wiley & Sons Inc.; 1955. 268 p.

[2] Bacon G. E. Neutron Diffraction. 3rd ed. Oxford: Claredon Press; 1975. 636 p.

[3] Gerold V., Kostorz G. Small-angle scattering applications to materials science. J. Appl. Cryst. 1978; 11: 376–404.

[4] Allen A. J., Windsor C. G., Rainey V., Pearson D., Double D. D., Alford N. M. A small angle neutron scattering study of cement porosities. J. Phys. D: Appl. Phys. 1982; 15: 1817–1833.

[5] Marshall W., Lovesey S. W. Theory of Thermal Neutron Scattering. 1st ed. Oxford: Claredon Press; 1971. 599 p.

[6] Kostorz G., editor. Treatise on Materials Science and Technology. 1st ed. New York: Academic Press; 1979. 523 p.

[7] Ostanevich Y. M. Time-of-flight small-angle scattering spectrometers on pulsed neutron sources. J. Makromol. Chem. 1988; 15: 91–103.